

# Systematic investigation of the nuclear multiple deformations in U+U collisions with A Multi-Phase Transport model

Zaining Wang,<sup>1,2</sup> Jinhui Chen,<sup>1,2,\*</sup> Hao-jie Xu,<sup>3,4,†</sup> and Jie Zhao<sup>1,2,‡</sup>

<sup>1</sup>Key Laboratory of Nuclear Physics and Ion-beam Application (MOE),  
Institute of Modern Physics, Fudan University, Shanghai 200433, China

<sup>2</sup>Shanghai Research Center for Theoretical Nuclear Physics,  
NSFC and Fudan University, Shanghai 200438, China

<sup>3</sup>School of Science, Huzhou University, Huzhou, Zhejiang 313000, China

<sup>4</sup>Strong-Coupling Physics International Research Laboratory (SPiRL), Huzhou University, Huzhou, Zhejiang 313000, China

(Dated: August 29, 2024)

Relativistic heavy ion collisions provide a unique opportunity to study the shape of colliding nuclei, even up to higher-order multiple deformations. In this work, several observables that are sensitive to quadrupole and hexadecapole deformations of Uranium-238 in relativistic U+U collisions have been systematically investigated with A Multi-Phase Transport model. We find that the flow harmonic  $v_2$ , the  $v_2$  and mean transverse momentum correlation, and the three-particle asymmetry cumulant  $ac_2\{3\}$  are sensitive to nuclear quadrupole deformation, while  $ac_2\{3\}$  and nonlinear response coefficient  $\chi_{4,22}$  are sensitive to nuclear hexadecapole deformation. Our results from transport model studies are in qualitative agreement with previous hydrodynamic studies. The results indicate that the uncertainties of the hexadecapole deformation of Uranium on the quadrupole deformation determination can be reduced by the abundance of correlation observables provided by the relativistic heavy ion collisions.

## I. INTRODUCTION

A deconfined quantum chromodynamics (QCD) medium, the so-called quark-gluon plasma (QGP), is believed to be formed within a few yoctoseconds ( $10^{-24}s$ ) in relativistic heavy ion collisions (HIC) at BNL's Relativistic Heavy Ion Collider (RHIC) and CERN's Large Hadron Collider (LHC) [1–5]. In HIC, the QCD strong interactions drive the initial geometry asymmetry of the QGP medium into an anisotropic distribution of final state hadrons in momentum space. Such an anisotropic momentum distribution can be described by flow harmonics  $v_n$  using Fourier expansions of the azimuthal distribution of the particles [6, 7]. The flow harmonics measured in relativistic HIC can be successfully described by relativistic hydrodynamics with the specific shear viscosity  $\eta/s$  close to the quantum lower limit  $1/4\pi$  [8–13]. In hydrodynamics, such a conversion is a consequence of the pressure gradient, and the hydrodynamic response of the lower order flow harmonics to the initial state is perfectly linear [14, 15], making it an ideal observable to trace back to spatial anisotropies in the initial state.

The spatial anisotropies of the QGP medium are governed by the impact parameter ( $b$ ) in non-head-on collisions [6], while they are dominated by the deformation of the colliding nuclei in most-central collisions ( $b \simeq 0$  fm) [16]. Several observables, such as the flow harmonics  $v_n$ , the mean transverse momentum fluctuations, and the flow harmonic correlations have been proposed to study the quadrupole ( $\beta_2$ ) and octupole deformations ( $\beta_3$ ) of the colliding nuclei in relativistic U+U collisions, Xe+Xe collisions, and isobar collisions [17–24].

The advantage of such an unconventional way to study the nuclear shape is that the nuclear structure is imprinted into the initial stage of the produced QGP with instant snapshots (yoctoseconds), mostly decoupled from the subsequent bulk evolution [16, 25–29]. Previous studies have focused on the lower-order nuclear multiple deformations, the heavy ion observables are expected to be less sensitive to the higher order deformations such as the hexadecapole deformations ( $\beta_4$ ), as their effect would be overwhelmed by that of the lower-order multiple deformations.

However, recent studies of relativistic U+U and Au+Au collisions indicate the importance of hexadecapole deformation in relativistic HIC [30–32]. The  $v_2$  differences between the most central U+U and Au+Au collisions measured at the top RHIC energy indicate that hydrodynamic simulations require either larger  $\beta_2$  for  $^{197}\text{Au}$  or smaller  $\beta_2$  for  $^{238}\text{U}$  than those commonly used in Woods-Saxon-type nuclear densities to describe the data [19, 20, 31, 32]. Such ambiguities cannot be avoided with the exact value of the ground state electrical transition rates  $B(E2) = 12.09 \pm 0.20 e^2 b^2$  of Uranium measured by the low-energy experiment [33], since the magnitude of  $\beta_2$  depends strongly on  $\beta_4$  for a given  $B(E2)$  [31, 34]. Considering the uncertainty of  $\beta_4$  in the low-energy experiment measurements and nuclear structure theory calculations, the observables proposed in relativistic HIC to extract the  $\beta_4$  of Uranium turn out to be meaningful [32].

In this study we consider a moderate uncertainty in the  $\beta_4$  of Uranium [35, 36], i.e.  $\beta_4 = 0.1$  vs.  $\beta_4 = 0$ , such an uncertainty gives  $\Delta\beta_2 \simeq 0.03$  for its quadrupole deformation uncertainty [31, 32]. The question is whether this uncertainty can be systematically reduced or eliminated by the observables obtained by relativistic HIC. The answer seems to be positive for the hydrodynamic simulations [32]. However, the discrepancy between the  $\beta_2$  of  $^{238}\text{U}$  extracted from  $v_2$  and other observables from hydrodynamic simulations [23] makes us think carefully about the uncertainties introduced by the models. Therefore,

\* chenjinhui@fudan.edu.cn

† haojiexu@zjhu.edu.cn

‡ jie.zhao@fudan.edu.cn

in this work, we use a transport model (A Multiphase Transport model AMPT) [37–40] to systematically investigate the observables that are sensitive to nuclear quadrupole and hexadecapole deformations in relativistic HIC. The AMPT model is generally considered to have a similar response to flow as hydrodynamics, while some other mechanisms, such as the anisotropic parton escape mechanism [41], are also proposed to be dramatically different from the hydrodynamic scenario.

The rest of the paper is organized as follows. Section II gives a brief description of the AMPT model and the definition of the observables used in this work. Section III discusses the effects of nuclear quadrupole and hexadecapole deformations on the flow-related observables in AMPT simulations. A summary is given in Sec. IV.

## II. MODEL SETUP AND ANALYSIS METHODS

### A. AMPT model

We perform all the calculations of the observables within AMPT model [37–40] to study the effects of different nuclear deformations on these observables in U+U collisions at  $\sqrt{s_{\text{NN}}} = 193$  GeV and Au+Au collisions at  $\sqrt{s_{\text{NN}}} = 200$  GeV. The AMPT model aims to apply the kinetic theory approach to describe the evolution of relativistic HIC as it contains four main components: the fluctuating initial conditions, partonic interactions, hadronization, and hadronic interactions [37]. It has since been widely used to simulate the evolution of the dense matter created in high-energy nuclear collisions. In particular, the string melting version of the AMPT model can well describe the anisotropic flows and particle correlations in collisions of  $pp$ ,  $pA$ , or  $AA$  systems at RHIC and LHC energies [42–51]. In our study, we use the string melting version of AMPT, and some of the key parameters are the Lund string fragmentation parameters  $a_L = 0.5$  and  $b_L = 0.9$  GeV<sup>-2</sup>, the parton screening mass  $\mu_D = 3.2032$  fm<sup>-1</sup>, and the strong coupling constant  $\alpha_S = 0.33$ , corresponding to a total cross section  $\sigma = 1.5$  mb. Since we focus on the nuclear deformation effect in most central collisions in this study, the AMPT with  $\sigma = 1.5$  mb was found to give better predictions on  $v_2$  and  $v_4$  in most central Au+Au collisions at  $\sqrt{s_{\text{NN}}} = 200$  GeV than those with  $\sigma = 3$  mb [52].

The shape of the nucleus with a finite number of nucleons distributed with a density  $\rho$  can be described by the Woods-Saxon distribution [53]

$$\rho(r, \theta) = \frac{\rho_0}{1 + \exp[(r - R)/a]}, \quad (1)$$

$$R = R_0(1 + \beta_2 Y_2^0(\theta) + \beta_4 Y_4^0(\theta)), \quad (2)$$

where  $R_0$  is the radius parameter,  $a$  is the diffuseness parameter,  $\beta_2$  and  $\beta_4$  are the deformation parameters, and  $Y_2^0$ ,  $Y_4^0$  are spherical harmonics. To study the uncertainties of  $\beta_2$  from  $\beta_4$ , we use three sets of parameters for <sup>238</sup>U with  $\Delta\beta_2 = 0.035$  and  $\Delta\beta_4 = 0.1$ , keeping other parameters same [31, 33, 54, 55]. The deformation parameters are listed in Tab I. Calculations of 0-60% centrality are performed and charged particles are

TABLE I. Deformation parameters applied in the AMPT model. Here we use Au + Au collisions as a reference in the computation of observables.

| Species | $R_0$ (fm) | $a$ (fm) | $\beta_2$ | $\beta_4$ |
|---------|------------|----------|-----------|-----------|
| a)      | 6.80       | 0.615    | 0.282     | 0.00      |
| U b)    | 6.80       | 0.615    | 0.247     | 0.10      |
| c)      | 6.80       | 0.615    | 0.282     | 0.10      |
| Au      | 6.38       | 0.535    | -0.131    | 0.00      |

selected with  $|\eta| < 2.0$  and  $p_T > 0.2$  GeV/c. To focus on the most central collisions, 3 million events with  $b_{\text{max}} = 20$  fm for each case and 1 million events with  $b_{\text{max}} = 4.74$  fm for U+U collisions are generated. The collision configurations are generated randomly with Euler rotations.

In this work, the flow harmonics  $v_n$ , the mean transverse momentum fluctuation, the Pearson correlation coefficient  $\rho(v_2^2, [p_T])$  between  $v_n$  and mean transverse momentum, three-particle asymmetry cumulant  $ac_2\{3\}$ , and the nonlinear response coefficient  $\chi_{4,22}$  between  $v_4$  and  $v_2$  in relativistic U+U collisions at  $\sqrt{s_{\text{NN}}} = 193$  GeV have been systematically investigated. We also use Au + Au collisions at  $\sqrt{s_{\text{NN}}} = 200$  GeV as a reference in the computation of observables, with their Woods-Saxon density parameters set to the commonly used values [56]. The results are shown as a ratio from U+U collisions to Au+Au collisions

$$R(X) \equiv \frac{X_{\text{UU}}}{X_{\text{AuAu}}}. \quad (3)$$

Before the discussion of the results, some definitions of these observables are given below.

### B. Observables

The azimuthal dependence of the final particle distribution can be written as

$$\frac{2\pi}{N} \frac{dN}{d\phi} = 1 + \sum_{n=1}^{\infty} 2v_n \cos n(\phi - \Psi_n). \quad (4)$$

Here  $v_n$  are the flow harmonics,  $\phi$  is the azimuthal angle of the momentum of the outgoing particles, and  $\Psi_n$  is the event plane angle [57] defined as  $\langle e^{in\phi} \rangle = v_n e^{in\Psi_n}$ , where  $\langle \dots \rangle$  is the average in a given event. The  $v_n(\Psi_n)$  can be calculated with the two-particle correlation method  $v_n\{2\}$ . In this work, the standard Q-cumulant method is used to calculate the flow observables [58].

For high order flow harmonics  $v_n$ , it can be calculated with respect to the lower-order event plane angle, not just the same order one  $\Psi_n$  [57]. For example, the  $v_4(\Psi_2)$  calculated with respect to the second-order event plane angular  $\Psi_2$  is directly related to the nonlinear part of  $v_4$  [59]

$$v_4\{2\} = v_4(\Psi_4) = v_{4L} + v_{4NL}, \quad (5)$$

$$v_{4NL} = v_4(\Psi_2) = \chi_{4,22}(v_2)^2, \quad (6)$$

where  $v_{4L}(v_{4NL})$  is the (non-)linear part of  $v_4$ , and  $\chi_{4,22}$  is the nonlinear response coefficient.

The three-particle asymmetry cumulant,

$$ac_2\{3\} \equiv \langle\langle 3 \rangle_{2,2,-4}\rangle = \langle v_2^4 \rangle^{1/2} v_4 \{ \Psi_2 \}, \quad (7)$$

reflects the flow harmonic correlation between  $v_2$  and  $v_4$  [22, 59–61]. Here  $\langle v_2^4 \rangle = \langle\langle 4 \rangle_{2,2,-2,-2}\rangle = 2v_2\{2\}^4 - v_2\{4\}^4$  denotes the four-particle moment, with the multiparticle azimuthal moment [58, 62] given by  $\langle m \rangle_{n_1, n_2, \dots, n_m} \equiv \langle e^{i(n_1 \varphi_{k_1} + n_2 \varphi_{k_2} + \dots + n_m \varphi_{k_m})} \rangle$ , where  $\langle \dots \rangle$  averages over all particles of interest (POI) in a given event, and an outer  $\langle\langle \dots \rangle\rangle$  denotes further average over an ensemble of events.  $ac_2\{3\}$  can be roughly written as [59]

$$ac_2\{3\} = \langle v_2^2 v_4 \cos 4(\Psi_4 - \Psi_2) \rangle. \quad (8)$$

The nonlinear response coefficient is then given by [32, 59],

$$\chi_{4,22} \equiv \frac{v_4 \{ \Psi_2 \}}{\langle v_2^4 \rangle^{1/2}} = \frac{ac_2\{3\}}{\langle v_2^4 \rangle}. \quad (9)$$

In hydrodynamic scenarios,  $ac_2\{3\}$  and  $\langle \cos 4(\Psi_4 - \Psi_2) \rangle$  are sensitive to  $\beta_2$  and  $\beta_3$ , while  $\chi_{4,22}$  can be considered an ideal observable to probe  $\beta_4$  as it is only sensitive to nuclear hexadecapole deformation [32].

The Pearson correlation coefficient  $\rho(v_2^2, [p_T])$  between  $v_2$  and the mean transverse momentum  $[p_T]$  is found to have a strong sensitivity to the nuclear deformations [63, 64], which can be calculated as

$$\rho(v_n^2, [p_T]) = \frac{\text{Cov}(v_n^2, [p_T])}{\sigma_{p_T} \sigma_{v_n^2}}, \quad (10)$$

where  $[p_T]$  is the averaged transverse momentum in a given event,  $\text{Cov}(v_n^2, [p_T])$  is the covariance between  $v_n^2$  and  $[p_T]$  and  $\sigma$  is the standard deviation. The deviation of  $v_n$  can be calculated by subtracting the four-particle correlation from the two-particle correlation. Besides  $\rho_2$ , the  $[p_T]$  variance  $\langle\langle (\delta p_T)^2 \rangle\rangle \equiv \sigma_{p_T}^2$  is also sensitive to nuclear deformation [65], where  $\delta p_T = [p_T] - \langle [p_T] \rangle_{\text{event}}$  is the fluctuation of  $[p_T]$  in a given centrality range and  $\langle \dots \rangle$  denotes the average over an ensemble of events.

### III. RESULTS AND DISCUSSIONS

Figure 1 shows the  $v_2\{2\}^2$  difference between U+U collisions and Au+Au collisions with different  $\beta_2$  and  $\beta_4$  of Uranium. The deformation effect is highlighted in the lower panel with the double ratios, where the contributions from the reference Au+Au collisions are canceled out. The quadrupole deformation has a significant contribution to  $v_2$  at most central collisions, and this feature has been found for decades [17]. We find that the  $v_2\{2\}^2$  at most central collisions can be clearly distinguished with  $\beta_2 = 0.282$  and  $\beta_2 = 0.247$  from the AMPT simulations. The small  $\beta_2$  of Uranium as a result of the suppression by  $\beta_4$  have been used to explain the  $R(v_2^2)$  data measured at RHIC [31], ignoring the uncertainties from the quadrupole deformation of gold. The effect of the hexadecapole deformation on  $v_2$  is relatively small, which is consistent with previous studies [32, 65].

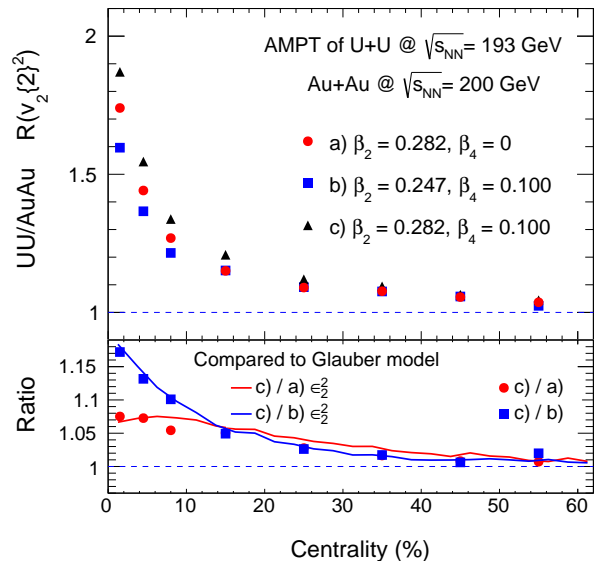


FIG. 1. (Color online) The ratios of the values of  $v_2\{2\}^2$  from U+U collisions to Au+Au collisions in the 0-60% centrality interval calculated from AMPT simulations. These cumulants are calculated by the standard Q-cumulant method using two-particle correlations. The bottom panel contains ratios of  $v_2^2$  from the AMPT model and  $\epsilon_2^2$  from the Monte Carlo Glauber model with different deformation parameters listed in Tab. I.

The AMPT model is known to have a similar response to the elliptic flow from medium expansion as hydrodynamics, i.e.,  $v_2 \propto \epsilon_2$  holds for most of the centrality [14, 15]. Therefore, the  $R(v_2\{2\}^2)$  can be well reproduced by the initial eccentricity ratio  $R(\epsilon_2^2)$ , where  $\epsilon_n e^{in\Phi_n} \equiv -\langle r^n e^{in\varphi} \rangle / \langle r^n \rangle$  with  $(r, \varphi)$  being the position of the participant in the transverse area and  $\Phi_n$  being the initial symmetry plane angle [14, 66]. Here  $\langle \dots \rangle$  denotes the averages over all participants. The double ratios of  $\epsilon_2^2$  obtained by a Monte Carlo Glauber simulation [56, 67] are also shown in the lower panel of Fig. 1. We confirm that the initial predictor  $\epsilon_2$  works well for all the centrality, as the results from AMPT and Monte Carlo Glauber simulations are almost overlapped. Due to the consistency among the macroscopic hydrodynamic model, the microscopic transport AMPT model, as well as the pure initial geometry Monte Carlo Glauber model, the nuclear quadrupole deformation extracted from elliptic flow ratio  $R(v_2\{2\}^2)$  between U+U collisions and Au+Au collisions is expected to have small model uncertainties. One ambiguity may be due to the hexadecapole deformation of the Uranium we have mentioned in the introduction [31], which cannot be well controlled by the elliptic flow data [32].

Besides the elliptic flow  $v_2$ , the mean transverse momentum fluctuation  $\langle\langle (\delta p_T)^2 \rangle\rangle$  and the Pearson correlation coefficient  $\rho(v_2^2, p_T)$  have also been used to extract the quadrupole deformation of the colliding nuclei [23, 63, 65]. The AMPT model is known to be a poor description of the mean transverse momentum and its fluctuation data, and some progress has been

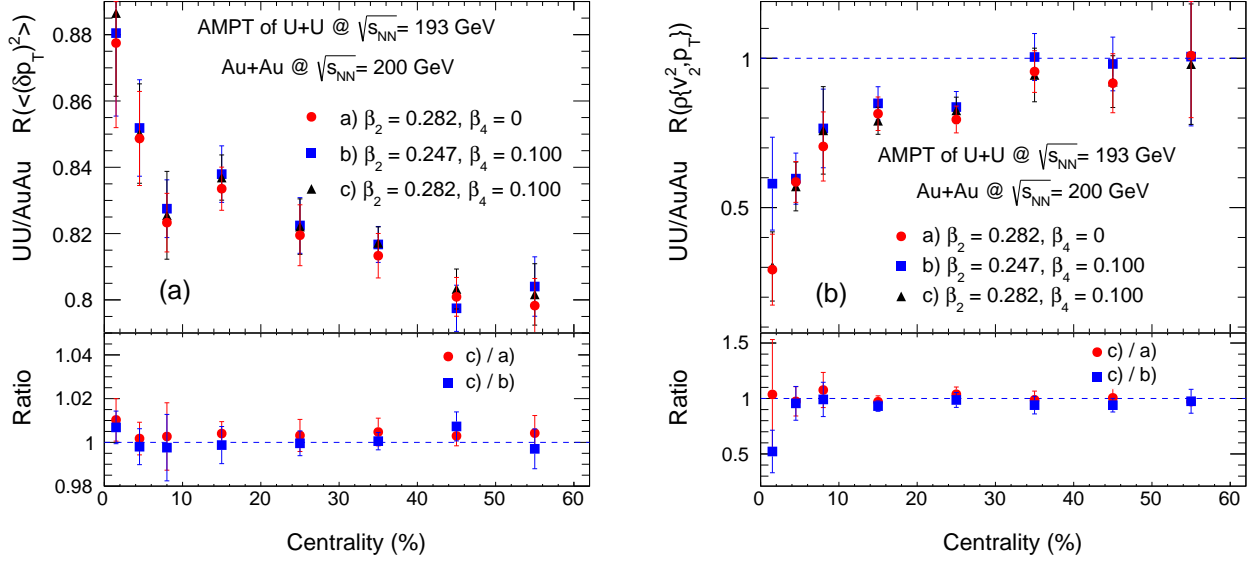


FIG. 2. (Color online) The ratios of the values of (a) the  $[p_T]$  variance  $\langle(\delta p_T)^2\rangle$  and (b) the Pearson correlation coefficient  $\rho(v_2^2, [p_T])$  of U+U collisions to Au+Au collisions calculated in the 0-60% centrality interval from AMPT simulations.

made on this issue [68–70]. Although with such drawback, it is worth investigating the deformation effect on  $\langle(\delta p_T)^2\rangle$  and  $\rho(v_2^2, p_T)$  differences between U+U collision and Au+Au collisions with AMPT simulations. The results are shown in Fig. 2. The deformation effect of both finite  $\beta_2$  difference and  $\beta_4$  difference on the  $[p_T]$  variance is invisible, see Fig. 2(a), in contrast to the conclusion from hydrodynamics [23]. Despite the absolute magnitudes, the  $R(\langle(\delta p_T)^2\rangle)$  shows a decreasing trend as a function of centrality, although much weaker, which is consistent with experimental data and hydrodynamic simulations [23].

Due to the limited statistics in our study, we cannot make a firm conclusion on the effect of nuclear deformation on  $\rho(v_2^2, p_T)$ , especially for the hexadecapole deformation. It appears that the quadrupole deformation gives large negative contribution to  $\rho(v_2^2, p_T)$  for most central collisions, and the hexadecapole deformation effect is negligible for all the centrality. These conclusions can be readily confirmed with more statistics. Moreover, the  $v_2$ - $p_T$  correlations are also found to be sensitive to triaxial deformation [71]. Due to the drawback of the current AMPT version, we propose such an AMPT study in the future. However, we note that the centrality-dependent trends of  $R(\rho(v_2^2, p_T))$  are in qualitative agreement with the experimental data and hydrodynamic simulations [23]. The deformation effect on  $\langle(\delta p_T)^2\rangle$  and  $\rho(v_2^2, p_T)$  has been studied in previous study using AMPT model with an even stronger partonic cross section  $\sigma = 3$  mb [65]. We expect that these results can be used to provide some insights into the improvement of the AMPT model [68, 69].

The observables discussed above are nearly insensitive to hexadecapole deformation. The effect of  $\beta_4$  on heavy ion observables is rarely studied, as it is typically overwhelmed by that of quadrupole deformations. Recent studies suggest that

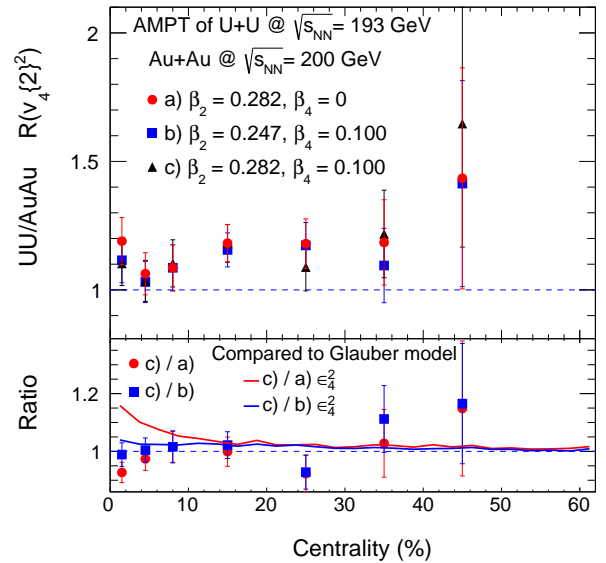


FIG. 3. (Color online) Similar to Fig. 1, but for the hexadecapole flow  $v_4\{2\}^2$  and  $\epsilon_4^2$ .

$\beta_4$  may play a very important role in explaining the elliptic flow difference between U+U collisions and Au+Au collisions [31]. Based on hydrodynamic simulations, several observables have been proposed to extract the value of  $\beta_4$  in relativistic HIC [32]. It is therefore worthwhile to test the sensitivity of these observables to  $\beta_4$  with a transport model simulation. In addition, the hydrodynamic response of the AMPT model to higher-order flow harmonics has not been extensively studied. Therefore,

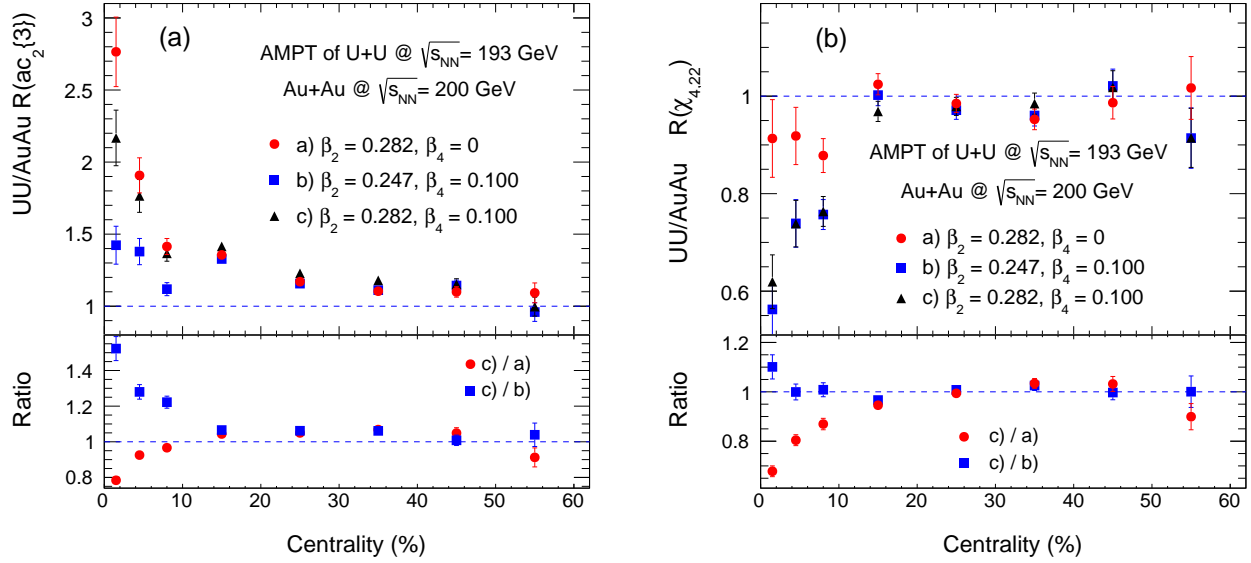


FIG. 4. (Color online) Similar to Fig. 2, but for (a) the three-particle asymmetry cumulant  $ac_2\{3\}$  and (b) the nonlinear response coefficient  $\chi_{4,22}$ .

we will focus on these  $\beta_4$ -sensitive observables that are related to the high-order flow harmonics in the rest of this paper.

Figure 3 presents the effect of  $\beta_2$  and  $\beta_4$  on the hexadecapole flow  $v_4$ . With the  $\beta_2$  and  $\beta_4$  differences discussed in this study, the quadrupole and hexadecapole deformation effects on  $v_4$  are negligibly small. This is not the case for the related initial predictor  $\epsilon_4$ . The  $\epsilon_4$  differences calculated with Monte Carlo Glauber simulations using the same nuclear deformation differences are also shown in the lower panel of Fig. 3. We find that the enhancement of  $\epsilon_4$  by  $\beta_4$  is obvious. The evolution driven by strong interactions not only distorts this enhancement but even gives a negative contribution to the final hexadecapole flow. This is similar to the results from hydrodynamic simulations [32]. The results indicate that the response of high order flow such as  $v_4$  in AMPT simulation is also non-diagonal and nonlinear [14].

The  $v_4$  is typically divided into the linear part  $v_{4L}$  and the nonlinear part  $v_{4NL}$  [59]. The three-particle asymmetry cumulant  $ac_2\{3\}$  is directly related to  $v_{4NL}$ , but more statistical friendly [22, 72]. The effect of nuclear deformation on  $ac_2\{3\}$  shown in Fig. 4(a) is quite obvious. The  $ac_2\{3\}$  increase with  $\beta_2$ , but decreases with  $\beta_4$ , in very good agreement with previous hydrodynamic simulations [32]. From Eq. 8, one would expect that the  $\beta_4$  dependence is roughly from the flow angle correlation  $\cos 4(\Psi_2 - \Psi_4)$ , as  $v_2$  and  $v_4$  are almost insensitive to  $\beta_4$  discussed before. This is confirmed by our AMPT simulations (not shown). The competition between  $\beta_2$  and  $\beta_4$  on  $ac_2\{3\}$  suggests that the extraction of  $\beta_2$  differences from  $ac_2\{3\}$  in relativistic HIC should be re-examined with the potential hexadecapole deformation of the colliding nuclei [22]. This would be an interesting topic for future work.

Previous studies with relativistic hydrodynamic simulations indicate that the nonlinear response coefficient  $\chi_{4,22}$  can be

considered as an ideal observable to extract the parameter  $\beta_4$  in relativistic HIC [32]. The effect of  $\beta_2$  and  $\beta_4$  on the nonlinear response coefficient  $\chi_{4,22}$  from the AMPT simulation is shown in Fig. 4(b). The  $\chi_{4,22}$  is significantly suppressed by the finite  $\beta_4$ , while the contributions from the finite  $\beta_2$  differences are reasonably small, in quantitative agreement with the predictions from hydrodynamic simulations [32]. The centrality dependence of  $R(\chi_{4,22})$  from AMPT simulations converge to units for non-central collisions, suggesting that differences in system size and/or nuclear quadrupole deformations have a negligible effect on  $\chi_{4,22}$ . The results indicate that the AMPT has a similar nonlinear response to high order flow harmonic  $v_4$  as hydrodynamics [32], making  $\chi_{4,22}$  as an ideal observable to probe nuclear hexadecapole deformations with small model uncertainties. Quantitatively, the effect of  $\beta_4$  on  $\chi_{4,22}$  is slightly ( $\sim 20\%$ ) weaker than the hydrodynamic response shown in Ref. [32]. These model uncertainties are crucial for the accurate extraction of  $\beta_4$  from relativistic HIC. Therefore, more precise investigations of the differences in the linear and nonlinear response of the hexadecapole flow between the transport model and the hydrodynamic model are required. We leave these investigations in the forthcoming paper but focus on a more ideal platform – relativistic isobar collisions [73–77].

In this paper, we focus mainly on the prediction differences between AMPT simulations and previous hydrodynamic simulations. We note that the differences in system sizes between U+U and Au+Au collisions may also have residual contributions to model uncertainties, despite the potential differences in response mechanisms between the transport and hydrodynamic models. One might expect that the ratios of the two systems would cancel out the uncertainties from the bulk evolution. This may be true for relativistic isobar collisions, but not for the case discussed in this study, since  $^{238}\text{U}$  and  $^{197}\text{Au}$

have almost  $\sim 20\%$  relative differences in mass number. The contributions from the non-flow would make the situation even worse [78, 79]. Therefore, although the hydrodynamic model is considered the "standard model" for high-energy HIC, a comprehensive understanding of the underlying physical differences between AMPT and hydrodynamics is crucial for the study of higher-order flow harmonics, especially for the proposal of accurate extraction of nuclear deformation parameters in relativistic HIC.

#### IV. SUMMARY

Anisotropic flows and their correlations in most central collisions are key observables to study the nuclear deformation effect in relativistic HIC. In this work, the flow harmonics  $v_2\{2\}$  and the related correlation observables such as the Pearson correlation coefficient  $\rho(v_2^2, [p_T])$  between the anisotropic flow and the mean transverse momentum, the three-particle asymmetry cumulant  $ac_2\{3\}$ , and the nonlinear response coefficient  $\chi_{4,22}$  between  $v_4$  and  $v_2$  in relativistic U+U collisions at  $\sqrt{s_{NN}} = 193$  GeV have been systematically studied with A Multiphase Transport model. We found that the former two observables  $v_2\{2\}$  and  $\rho(v_2^2, [p_T])$  are sensitive to quadrupole deformation, while the latter one  $\chi_{4,22}$  is mostly sensitive to hexadecapole deformation. The  $ac_2\{3\}$  is sensitive to both quadrupole and hexadecapole deformations. These features

are in qualitative agreement with the results from hydrodynamic simulations. Due to the incorrect response of the radial flow, the  $[p_T]$  variance in AMPT simulations is insensitive to nuclear deformation, in contrast to the hydrodynamic scenario. Our results suggest that  $v_2$  ( $\chi_{4,22}$ ) can be considered as an ideal observable to extract the nuclear quadrupole (hexadecapole) deformation parameter with small model uncertainties, although these uncertainties need to be investigated in detail for more precise constraints. The results indicate that the uncertainty of the  $\beta_2$  measurement introduced by the unknown hexadecapole deformation can be largely reduced by more deformation-sensitive observables in relativistic HIC.

#### ACKNOWLEDGEMENTS.

We thank Zi-Wei Lin for providing the AMPT code and for fruitful discussions. This work was supported in part by the National Key Research and Development Program of China under Contract No. 2022YFA1604900, by the National Natural Science Foundation of China (NSFC) under Contract No. 12025501, No. 12035006, No. 12075085, No. 12147101, No. 12275082, No. 12275053, by the Strategic Priority Research Program of Chinese Academy of Sciences under Grant No. XDB34030000, and by the Guangdong Major Project of Basic and Applied Basic Research No. 2020B0301030008.

- 
- [1] E. V. Shuryak, Quantum Chromodynamics and the Theory of Superdense Matter, *Phys. Rept.* **61**, 71 (1980).
- [2] J. Adams *et al.* (STAR Collaboration), Experimental and theoretical challenges in the search for the quark gluon plasma: The STAR Collaboration's critical assessment of the evidence from RHIC collisions, *Nucl.Phys.* **A757**, 102 (2005), arXiv:nucl-ex/0501009 [nucl-ex].
- [3] K. Adcox *et al.* (PHENIX Collaboration), Formation of dense partonic matter in relativistic nucleus-nucleus collisions at RHIC: Experimental evaluation by the PHENIX collaboration, *Nucl.Phys.* **A757**, 184 (2005), arXiv:nucl-ex/0410003 [nucl-ex].
- [4] K. Aamodt *et al.* (ALICE), Elliptic flow of charged particles in Pb-Pb collisions at 2.76 TeV, *Phys. Rev. Lett.* **105**, 252302 (2010), arXiv:1011.3914 [nucl-ex].
- [5] J. Chen *et al.*, Properties of the QCD Matter – An Experimental Review of Selected Results from RHIC BES Program, (2024), arXiv:2407.02935 [nucl-ex].
- [6] J.-Y. Ollitrault, Anisotropy as a signature of transverse collective flow, *Phys. Rev. D* **46**, 229 (1992).
- [7] P. F. Kolb, P. Huovinen, U. W. Heinz, and H. Heiselberg, Elliptic flow at SPS and RHIC: From kinetic transport to hydrodynamics, *Phys. Lett.* **B500**, 232 (2001), arXiv:hep-ph/0012137 [hep-ph].
- [8] P. Kovtun, D. Son, and A. Starinets, Viscosity in strongly interacting quantum field theories from black hole physics, *Phys.Rev.Lett.* **94**, 111601 (2005), arXiv:hep-th/0405231 [hep-th].
- [9] P. Romatschke and U. Romatschke, Viscosity Information from Relativistic Nuclear Collisions: How Perfect is the Fluid Observed at RHIC?, *Phys.Rev.Lett.* **99**, 172301 (2007), arXiv:0706.1522 [nucl-th].
- [10] H. Song, S. A. Bass, U. Heinz, T. Hirano, and C. Shen, 200 A GeV Au+Au collisions serve a nearly perfect quark-gluon liquid, *Phys. Rev. Lett.* **106**, 192301 (2011), [Erratum: *Phys. Rev. Lett.* **109**, 139904(2012)], arXiv:1011.2783 [nucl-th].
- [11] C. Shen and L. Yan, Recent development of hydrodynamic modeling in heavy-ion collisions, *Nucl. Sci. Tech.* **31**, 122 (2020), arXiv:2010.12377 [nucl-th].
- [12] M. Wang, J.-Q. Tao, H. Zheng, W.-C. Zhang, L.-L. Zhu, and A. Bonasera, Number-of-constituent-quark scaling of elliptic flow: a quantitative study, *Nucl. Sci. Tech.* **33**, 37 (2022), arXiv:2203.10353 [hep-ph].
- [13] X.-G. Deng, D.-Q. Fang, and Y.-G. Ma, Shear viscosity of nucleonic matter, *Prog. Part. Nucl. Phys.* **136**, 104095 (2024), arXiv:2401.02293 [nucl-th].
- [14] Z. Qiu and U. W. Heinz, Event-by-event shape and flow fluctuations of relativistic heavy-ion collision fireballs, *Phys. Rev. C* **84**, 024911 (2011), arXiv:1104.0650 [nucl-th].
- [15] D.-X. Wei, X.-G. Huang, and L. Yan, Hydrodynamic response in simulations within a multiphase transport model, *Phys. Rev. C* **98**, 044908 (2018), arXiv:1807.06299 [nucl-th].
- [16] J. Jia, Shape of atomic nuclei in heavy ion collisions, *Phys. Rev. C* **105**, 014905 (2022), arXiv:2106.08768 [nucl-th].
- [17] U. W. Heinz and A. Kuhlman, Anisotropic flow and jet quenching in ultrarelativistic U + U collisions, *Phys. Rev. Lett.* **94**, 132301 (2005), arXiv:nucl-th/0411054.
- [18] X.-F. Luo, X. Dong, M. Shao, K.-J. Wu, C. Li, and H.-F. Chen, Stopping effects in U + U collisions with a beam energy of 520-MeV/nucleon, *Phys. Rev. C* **76**, 044902 (2007), arXiv:0704.0424 [nucl-ex].

- [19] B. Schenke, C. Shen, and P. Tribedy, Running the gamut of high energy nuclear collisions, *Phys. Rev. C* **102**, 044905 (2020), arXiv:2005.14682 [nucl-th].
- [20] G. Giacalone, J. Jia, and C. Zhang, Impact of Nuclear Deformation on Relativistic Heavy-Ion Collisions: Assessing Consistency in Nuclear Physics across Energy Scales, *Phys. Rev. Lett.* **127**, 242301 (2021), arXiv:2105.01638 [nucl-th].
- [21] N. Magdy, Impact of nuclear deformation on collective flow observables in relativistic U+U collisions, *Eur. Phys. J. A* **59**, 64 (2023), arXiv:2206.05332 [nucl-th].
- [22] S. Zhao, H.-j. Xu, Y.-X. Liu, and H. Song, Probing the nuclear deformation with three-particle asymmetric cumulant in RHIC isobar runs, *Phys. Lett. B* **839**, 137838 (2023), arXiv:2204.02387 [nucl-th].
- [23] STAR *et al.* (STAR), Imaging Shapes of Atomic Nuclei in High-Energy Nuclear Collisions, (2024), arXiv:2401.06625 [nucl-ex].
- [24] G. Aad *et al.* (ATLAS), Correlations between flow and transverse momentum in Xe+Xe and Pb+Pb collisions at the LHC with the ATLAS detector: A probe of the heavy-ion initial state and nuclear deformation, *Phys. Rev. C* **107**, 054910 (2023), arXiv:2205.00039 [nucl-ex].
- [25] S. Zhang, Y. G. Ma, J. H. Chen, W. B. He, and C. Zhong, Nuclear cluster structure effect on elliptic and triangular flows in heavy-ion collisions, *Phys. Rev. C* **95**, 064904 (2017), arXiv:1702.02507 [nucl-th].
- [26] H. Li, H.-j. Xu, Y. Zhou, X. Wang, J. Zhao, L.-W. Chen, and F. Wang, Probing the neutron skin with ultrarelativistic isobaric collisions, *Phys. Rev. Lett.* **125**, 222301 (2020), arXiv:1910.06170 [nucl-th].
- [27] H.-j. Xu, W. Zhao, H. Li, Y. Zhou, L.-W. Chen, and F. Wang, Probing nuclear structure with mean transverse momentum in relativistic isobar collisions, *Phys. Rev. C* **108**, L011902 (2023), arXiv:2111.14812 [nucl-th].
- [28] J.-f. Wang, H.-j. Xu, and F. Wang, Impact of initial fluctuations and nuclear deformations in isobar collisions, (2023), arXiv:2305.17114 [nucl-th].
- [29] Y. Wang, S. Zhao, B. Cao, H.-j. Xu, and H. Song, Exploring the compactness of  $\alpha$  clusters in O16 nuclei with relativistic O16+O16 collisions, *Phys. Rev. C* **109**, L051904 (2024), arXiv:2401.15723 [nucl-th].
- [30] L. Adamczyk *et al.* (STAR), Azimuthal anisotropy in U+U and Au+Au collisions at RHIC, *Phys. Rev. Lett.* **115**, 222301 (2015), arXiv:1505.07812 [nucl-ex].
- [31] W. Ryssens, G. Giacalone, B. Schenke, and C. Shen, Evidence of Hexadecapole Deformation in Uranium-238 at the Relativistic Heavy Ion Collider, *Phys. Rev. Lett.* **130**, 212302 (2023), arXiv:2302.13617 [nucl-th].
- [32] H.-j. Xu, J. Zhao, and F. Wang, Hexadecapole deformation of  $^{238}\text{U}$  from relativistic heavy-ion collisions using a non-linear response coefficient, *Phys. Rev. Lett.* **in press** (2024), arXiv:2402.16550 [nucl-th].
- [33] S. Raman, C. W. G. Nestor, Jr, and P. Tikkanen, Transition probability from the ground to the first-excited 2+ state of even-even nuclides, *Atom. Data Nucl. Data Tabl.* **78**, 1 (2001).
- [34] W. Ryssens, V. Hellemans, M. Bender, and P. H. Heenen, Solution of the Skyrme-HF+BCS equation on a 3D mesh, II: A new version of the Ev8 code, *Comput. Phys. Commun.* **187**, 175 (2015), arXiv:1405.1897 [nucl-th].
- [35] C. E. Bemis, F. K. McGowan, J. L. C. Ford, W. T. Milner, P. H. Stelson, and R. L. Robinson, E-2 and E-4 Transition Moments and Equilibrium Deformations in the Actinide Nuclei, *Phys. Rev. C* **8**, 1466 (1973).
- [36] J. D. Zumbro, E. B. Shera, Y. Tanaka, C. E. Bemis, R. A. Naumann, M. V. Hoehn, W. Reuter, and R. M. Steffen, E-2 and E-4 Deformations in U-233, U-234, U-235, U-238, *Phys. Rev. Lett.* **53**, 1888 (1984).
- [37] Z.-W. Lin, C. M. Ko, B.-A. Li, B. Zhang, and S. Pal, A Multiphase transport model for relativistic heavy ion collisions, *Phys. Rev. C* **72**, 064901 (2005), arXiv:nucl-th/0411110.
- [38] X.-N. Wang and M. Gyulassy, HIJING: A Monte Carlo model for multiple jet production in p p, p A and A A collisions, *Phys. Rev. D* **44**, 3501 (1991).
- [39] B.-A. Li and C. M. Ko, Formation of superdense hadronic matter in high-energy heavy ion collisions, *Phys. Rev.* **C52**, 2037 (1995), arXiv:nucl-th/9505016 [nucl-th].
- [40] B. Zhang, ZPC 1.0.1: A Parton cascade for ultrarelativistic heavy ion collisions, *Comput. Phys. Commun.* **109**, 193 (1998), arXiv:nucl-th/9709009 [nucl-th].
- [41] L. He, T. Edmonds, Z.-W. Lin, F. Liu, D. Molnar, and F. Wang, Anisotropic parton escape is the dominant source of azimuthal anisotropy in transport models, *Phys. Lett. B* **753**, 506 (2016), arXiv:1502.05572 [nucl-th].
- [42] A. Bzdak and G.-L. Ma, Elliptic and triangular flow in  $p$ +Pb and peripheral Pb+Pb collisions from parton scatterings, *Phys. Rev. Lett.* **113**, 252301 (2014), arXiv:1406.2804 [hep-ph].
- [43] S. Zhang, Y. G. Ma, G. L. Ma, J. H. Chen, Q. Y. Shou, W. B. He, and C. Zhong, Collision system size scan of collective flows in relativistic heavy-ion collisions, *Phys. Lett. B* **804**, 135366 (2020), arXiv:2003.06747 [nucl-th].
- [44] Y.-A. Li, D.-F. Wang, S. Zhang, and Y.-G. Ma, System evolution of forward-backward multiplicity correlations in a multiphase transport model, *Phys. Rev. C* **104**, 044906 (2021), arXiv:2110.04784 [hep-ph].
- [45] D. Shen, J. Chen, and Z.-W. Lin, The effect of hadronic scatterings on the measurement of vector meson spin alignments in heavy-ion collisions, *Chin. Phys. C* **45**, 054002 (2021), arXiv:2102.05266 [nucl-ex].
- [46] L. Zhang, J. Chen, W. Li, and Z.-W. Lin, Implication of two-baryon azimuthal correlations in pp collisions at LHC energies on the QGP, *Phys. Lett. B* **829**, 137063 (2022), arXiv:2112.14358 [hep-ph].
- [47] H. Wang and J.-H. Chen, Anisotropy flows in Pb-Pb collisions at LHC energies from parton scatterings with heavy quark trigger, *Nucl. Sci. Tech.* **33**, 15 (2022).
- [48] T. Shao, J. Chen, Y.-G. Ma, and Z. Xu, Production of light antinuclei in pp collisions by dynamical coalescence and their fluxes in cosmic rays near earth, *Phys. Rev. C* **105**, 065801 (2022), arXiv:2205.13626 [hep-ph].
- [49] L.-L. Zhu, B. Wang, M. Wang, and H. Zheng, Energy and centrality dependence of light nuclei production in relativistic heavy-ion collisions, *Nucl. Sci. Tech.* **33**, 45 (2022).
- [50] X.-L. Zhao, Z.-W. Lin, L. Zheng, and G.-L. Ma, A transport model study of multiparticle cumulants in p+p collisions at 13 TeV, *Phys. Lett. B* **839**, 137799 (2023), arXiv:2112.01232 [nucl-th].
- [51] D. Shen, J. Chen, A. Tang, and G. Wang, Impact of globally spin-aligned vector mesons on the search for the chiral magnetic effect in heavy-ion collisions, *Phys. Lett. B* **839**, 137777 (2023), arXiv:2212.03056 [nucl-th].
- [52] M. Nasim, Systematic study of symmetric cumulants at  $\sqrt{s_{NN}} = 200$  GeV in Au+Au collision using transport approach, *Phys. Rev. C* **95**, 034905 (2017), arXiv:1612.01066 [nucl-ex].
- [53] R. D. Woods and D. S. Saxon, Diffuse Surface Optical Model for Nucleon-Nuclei Scattering, *Phys. Rev.* **95**, 577 (1954).
- [54] H. De Vries, C. W. De Jager, and C. De Vries, Nuclear charge and magnetization density distribution parameters from elastic

- electron scattering, *Atom. Data Nucl. Data Tabl.* **36**, 495 (1987).
- [55] B. Pritychenko, M. Birch, B. Singh, and M. Horoi, Tables of E2 Transition Probabilities from the first  $2^+$  States in Even-Even Nuclei, *Atom. Data Nucl. Data Tabl.* **107**, 1 (2016), [Erratum: *Atom. Data Nucl. Data Tabl.* 114, 371–374 (2017)], arXiv:1312.5975 [nucl-th].
- [56] C. Loizides, J. Kamin, and D. d’Enterria, Improved Monte Carlo Glauber predictions at present and future nuclear colliders, *Phys. Rev. C* **97**, 054910 (2018), [Erratum: *Phys. Rev. C* 99, 019901 (2019)], arXiv:1710.07098 [nucl-ex].
- [57] A. M. Poskanzer and S. A. Voloshin, Methods for analyzing anisotropic flow in relativistic nuclear collisions, *Phys. Rev. C* **58**, 1671 (1998), arXiv:nucl-ex/9805001.
- [58] A. Bilandzic, R. Snellings, and S. Voloshin, Flow analysis with cumulants: Direct calculations, *Phys. Rev. C* **83**, 044913 (2011), arXiv:1010.0233 [nucl-ex].
- [59] L. Yan and J.-Y. Ollitrault,  $v_4, v_5, v_6, v_7$ : nonlinear hydrodynamic response versus LHC data, *Phys. Lett. B* **744**, 82 (2015), arXiv:1502.02502 [nucl-th].
- [60] G. Aad *et al.* (ATLAS), Measurement of long-range pseudorapidity correlations and azimuthal harmonics in  $\sqrt{s_{NN}} = 5.02$  TeV proton-lead collisions with the ATLAS detector, *Phys. Rev. C* **90**, 044906 (2014), arXiv:1409.1792 [hep-ex].
- [61] J. Jia, M. Zhou, and A. Trzupek, Revealing long-range multiparticle collectivity in small collision systems via subevent cumulants, *Phys. Rev. C* **96**, 034906 (2017), arXiv:1701.03830 [nucl-th].
- [62] A. Bilandzic, C. H. Christensen, K. Gulbrandsen, A. Hansen, and Y. Zhou, Generic framework for anisotropic flow analyses with multiparticle azimuthal correlations, *Phys. Rev. C* **89**, 064904 (2014), arXiv:1312.3572 [nucl-ex].
- [63] G. Giacalone, Constraining the quadrupole deformation of atomic nuclei with relativistic nuclear collisions, *Phys. Rev. C* **102**, 024901 (2020), arXiv:2004.14463 [nucl-th].
- [64] J. Jia, S. Huang, and C. Zhang, Probing nuclear quadrupole deformation from correlation of elliptic flow and transverse momentum in heavy ion collisions, *Phys. Rev. C* **105**, 014906 (2022), arXiv:2105.05713 [nucl-th].
- [65] J. Jia, Probing triaxial deformation of atomic nuclei in high-energy heavy ion collisions, *Phys. Rev. C* **105**, 044905 (2022), arXiv:2109.00604 [nucl-th].
- [66] X. Zhu, Y. Zhou, H. Xu, and H. Song, Correlations of flow harmonics in 2.76A TeV Pb–Pb collisions, *Phys. Rev. C* **95**, 044902 (2017), arXiv:1608.05305 [nucl-th].
- [67] M. L. Miller, K. Reygers, S. J. Sanders, and P. Steinberg, Glauber modeling in high energy nuclear collisions, *Ann. Rev. Nucl. Part. Sci.* **57**, 205 (2007), arXiv:nucl-ex/0701025 [nucl-ex].
- [68] Z.-W. Lin and L. Zheng, Further developments of a multi-phase transport model for relativistic nuclear collisions, *Nucl. Sci. Tech.* **32**, 113 (2021), arXiv:2110.02989 [nucl-th].
- [69] C. Zhang, L. Zheng, S. Shi, and Z.-W. Lin, Using local nuclear scaling of initial condition parameters to improve the system size dependence of transport model descriptions of nuclear collisions, *Phys. Rev. C* **104**, 014908 (2021), arXiv:2103.10815 [nucl-th].
- [70] X.-L. Zhao, G.-L. Ma, Y. Zhou, Z.-W. Lin, and C. Zhang, Nuclear cluster structure effect in  $^{16}\text{O}+^{16}\text{O}$  collisions at the top RHIC energy, (2024), arXiv:2404.09780 [nucl-th].
- [71] B. Bally, M. Bender, G. Giacalone, and V. Somà, Evidence of the triaxial structure of  $^{129}\text{Xe}$  at the Large Hadron Collider, *Phys. Rev. Lett.* **128**, 082301 (2022), arXiv:2108.09578 [nucl-th].
- [72] C. Zhang, J. Jia, and J. Xu, Non-flow effects in three-particle mixed-harmonic azimuthal correlations in small collision systems, *Phys. Lett. B* **792**, 138 (2019), arXiv:1812.03536 [nucl-th].
- [73] W.-T. Deng, X.-G. Huang, G.-L. Ma, and G. Wang, Test the chiral magnetic effect with isobaric collisions, *Phys. Rev. C* **94**, 041901 (2016), arXiv:1607.04697 [nucl-th].
- [74] H.-J. Xu, X. Wang, H. Li, J. Zhao, Z.-W. Lin, C. Shen, and F. Wang, Importance of isobar density distributions on the chiral magnetic effect search, *Phys. Rev. Lett.* **121**, 022301 (2018), arXiv:1710.03086 [nucl-th].
- [75] H.-j. Xu, H. Li, X. Wang, C. Shen, and F. Wang, Determine the neutron skin type by relativistic isobaric collisions, *Phys. Lett. B* **819**, 136453 (2021), arXiv:2103.05595 [nucl-th].
- [76] C. Zhang and J. Jia, Evidence of Quadrupole and Octupole Deformations in Zr96+Zr96 and Ru96+Ru96 Collisions at Ultrarelativistic Energies, *Phys. Rev. Lett.* **128**, 022301 (2022), arXiv:2109.01631 [nucl-th].
- [77] M. Abdallah *et al.* (STAR), Search for the chiral magnetic effect with isobar collisions at  $\sqrt{s_{NN}}=200$  GeV by the STAR Collaboration at the BNL Relativistic Heavy Ion Collider, *Phys. Rev. C* **105**, 014901 (2022), arXiv:2109.00131 [nucl-ex].
- [78] N. Borghini, P. M. Dinh, and J.-Y. Ollitrault, Are flow measurements at SPS reliable?, *Phys. Rev. C* **62**, 034902 (2000), arXiv:nucl-th/0004026 [nucl-th].
- [79] Q. Wang and F. Wang, Non-flow correlations in a cluster model, *Phys. Rev. C* **81**, 064905 (2010), arXiv:0812.1176 [nucl-ex].